

Proton-bound dimers of 1-methylcytosine and its derivatives: vibrational and NMR spectroscopy†

Cite this: *Phys. Chem. Chem. Phys.*, 2013, **15**, 19001

Hou U. Ung,^a Aaron R. Moehlig,^{†ab} Ryan A. Kudla,^a Leonard J. Mueller,^a Jos Oomens,^{cd} Giel Berden^c and Thomas Hellman Morton^{*a}

Vibrational spectroscopy and NMR demonstrate that the proton-bound dimer of 1-methylcytosine, **1**, has an unsymmetrical structure at room temperature. In the gas phase, investigation of isolated homodimer **1** reveals five fundamental NH vibrations by IR Multiple Photon Dissociation (IRMPD) action spectroscopy. The NH...N stretching vibration between the two ring nitrogens exhibits a frequency of 1570 cm⁻¹, as confirmed by examination of the proton-bound homodimers of 5-fluoro-1-methylcytosine, **2**, and of 1,5-dimethylcytosine, **3**, which display absorptions in the same region that disappear upon deuterium substitution. ¹³C, and ¹⁵N NMR of the solid iodide salt of **1** confirm the nonequivalence of the two rings in the anhydrous proton-bound homodimer at room temperature. IRMPD spectra of the three possible heterodimers also show NH...N stretches in the same domain, and at least one of the heterodimers, the proton-bound dimer of 1,5-dimethylcytosine with 1-methylcytosine, exhibits two bands suggestive of the presence of two tautomers close in energy.

Received 29th May 2013,
Accepted 24th September 2013

DOI: 10.1039/c3cp52260a

www.rsc.org/pccp

Introduction

Dimerization of nucleobases by H⁺ bridging represents a non-Watson–Crick form of association whose biological relevance has emerged in recent years. Many questions remain regarding the structure and dynamics of the proton bridge. This paper presents an examination of proton-bound dimers of 1-methylcytosine and its derivatives using several approaches – solid state NMR (ssNMR), vibrational spectroscopy, X-ray diffraction, and computation – in order to answer two questions. First, is the bridging proton shared equally by both bases in the equilibrium geometry? Second, does a normal modes treatment

provide a suitable approximation to describe the vibrational structure? As presented below, the experimental data provide negative answers to both questions.

Background

Single strand self association within DNA has been recognized only comparatively recently as pertinent to biological processes.¹ Patterns of self association between identical bases include the i-motif, which consists of proton-bound dimers of cytosine intercalated with one another,^{2–4} and G-quadplexes, which bind the Watson–Crick face of one purine to the Hoogsteen face of another.¹ Fig. 1A schematically depicts the intercalation of proton-bound deoxyC dimers (also called hemiprotonated C-dimers, represented by ellipses) within a single strand in the i-motif, while Fig. 1B represents the proton-bridged association of the two Watson–Crick faces of a pair of cytosine residues within each ellipse.

Schwalbe and coworkers recently published a detailed analysis of the i-motif structure of a 21-deoxynucleotide C-rich repeat unit from telomeric DNA.² By means of NMR of labeled single strands, as well as circular dichroism (CD) and other techniques, they uncover a number of important structural features of the i-motif, such as the equilibrium and rates of interconversion between isomeric forms. Intermolecular association of oligo-C strands has also been demonstrated by CD studies, which give an idea of how many bases are needed to overcome the entropic barrier to H⁺-promoted pairing.³

^a Department of Chemistry, University of California, Riverside, CA 92521-0403, USA. E-mail: morton@citrus.ucr.edu

^b Laboratoire de Pharmacognosie – UMR BIOCIS, Université Paris-Sud XI, Faculté de Pharmacie, 5, rue Jean-Baptiste Clément, 92296 Châtenay-Malabry, France

^c Radboud University Nijmegen, Institute for Molecules and Materials, FELIX Facility, Toernooiveld 7, NL-6525ED Nijmegen, The Netherlands

^d van't Hoff Institute for Molecular Sciences, University of Amsterdam, Science Park 904, NL-1098XH, The Netherlands

† Electronic supplementary information (ESI) available: IRMPD spectrum of the *d*₄-homodimer of 1-methyl-*d*₃-cytosine; IRMPD spectra of **1–6** with tabulated assignments; ¹H solid state of the iodide salt of **1**; DFT-calculated ¹³C and ¹⁵N chemical shifts of **1**; comparisons of IR absorption spectrum of the iodide salt of **1** with the gas IRMPD spectrum of gaseous **1**, of the IR absorption spectra of crystal habit A with crystal habit B of the iodide salt of **1**, and of the IR powder absorption spectra of the *d*₅-exchanged iodide salt of **1** with the unexchanged salt. See DOI: 10.1039/c3cp52260a

† Current address: Department of Chemistry, Adams State University, Alamosa, CO 81101 USA.

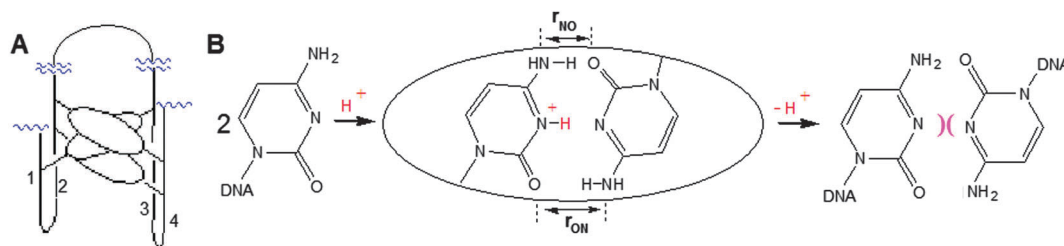


Fig. 1 (A) Schematic depiction of intrastrand stacking of three proton-bound cytosine dimers within the i-motif, which alternates dimers (represented as ellipses) from regions 1 and 3 with dimers from regions 2 and 4. (B) Association of two cytosines in a parallel orientation promoted by binding a proton between them. Two hydrogen bonds flank the ionic hydrogen bond between the ring nitrogens, with unequal N–O distances r_{NO} and r_{ON} , as validated by nearly all published crystallographic structures as well as the spectra reproduced below. Deprotonation leads to net repulsion between the two rings (represented by) (to the far right).

Recent work raises the possibility that intrastrand association takes place not only at the ends of chromosomes (the telomeric region) but also within double helical domains deep inside duplex DNA. Such aggregation requires that C.G-rich regions of the Watson–Crick duplex separate from one another and form the i-motif and a G-quadruplex, respectively. One model proposes that promoters of genes such as *c-Myc* or *VEGF* undergo such a conformational change while underwound and that this influences transcription.⁴

Many crystallographic structures of the proton-bound dimer of cytosine and its derivatives have been published,^{5–7} as well as of a number of aggregates of C-rich oligonucleotides that bind together *via* the i-motif.^{8,9} Association of *N*-substituted cytosines with their conjugate acids has recently been demonstrated in solution, as well.¹⁰ On the one hand, the majority of crystal structures show that the distances r_{NO} and r_{ON} shown in Fig. 1 differ by between 0.15 and 0.2 Å in the equilibrium geometry, consistent with the solid phase NMR spectra reported below. On the other hand, calculations suggest that proton transfer from one base to the other should occur easily, interchanging the two distances.¹¹ The calculated barrier for the proton-bound dimer of cytosine does appear to have a value higher than that for the proton-bound dimer of 8-aminopurine, for which theory predicts a low-barrier ionic hydrogen bond.¹²

Published data do not unambiguously resolve the question of the symmetry of hemiprotonated cytosines at room temperature. The barrier may depend on environment and the identity of the counterion. A careful X-ray investigation by Bošnjaković-Pavlović and Spasajević-de Biré reveals a temperature-dependent example.⁷ Above 200 K the decavanadate salt of the proton-bound dimer of cytosine possesses an inversion point of symmetry, meaning that r_{NO} has the same value as r_{ON} , but at 100 K the symmetry vanishes. In another case, the two nitrogen–oxygen distances become nearly equal in the middle of a tetrameric stack of proton-bound oligodeoxynucleotides, but not at the ends.⁹

The literature does not contain much detail regarding the vibrational structure of proton-bound dimers of cytosine. The only band characteristic of the proton-bound dimer has been reported to occur at 1890 cm^{-1} ,¹³ which lies outside the domain of the gas phase experiments described below. The recently developed ability to take IR spectra of organic ions in the gas phase¹⁴ has greatly increased knowledge of ionic hydrogen bonding.^{15,16} Our preliminary communication regarding the proton-bound dimer of 1-methylcytosine in the fingerprint region ($300\text{--}1800\text{ cm}^{-1}$) shows a feature at 1570 cm^{-1} that we have assigned to the motion of the bridging proton from one base to the other.¹⁷ The present work exhibits the same band in the substituted 1-methylcytosine homo- and heterodimers depicted in Chart 1, which

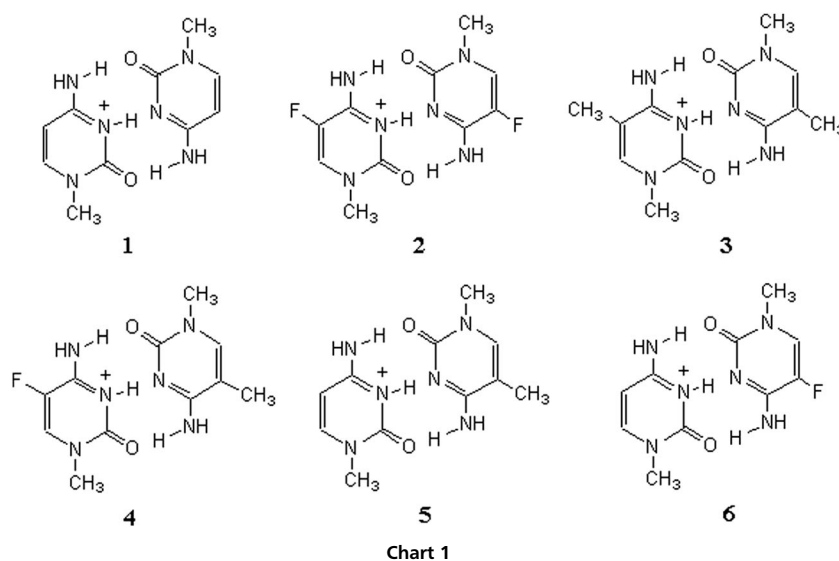


Chart 1

provides a confirmation of this assignment. In heterodimers, where the two bases have proton affinities close to one another, the band appears to be doubled, possibly indicating the presence of two tautomers.

Experimental section

1-Methylcytosine was prepared as described in the literature.¹⁸ 5-Fluoro-1-methyl-cytosine and 1,5-dimethylcytosine were prepared from commercially available 5-fluorocytosine and 5-methylcytosine, respectively, using the same procedure. Crystalline samples of the iodide salt of **1** were prepared by adding 0.5 equivalents of 47% aqueous hydrogen iodide to a saturated solution of 1-methylcytosine in absolute ethanol, removal of solvent by distillation under reduced pressure, and recrystallization of the resulting solid 7 times from absolute ethanol. After repeated recrystallizations the mixture of polymorphs resolved principally into crystal habit B, fine needles whose solid phase NMR spectra are reproduced in Fig. 2 and in the ESI.† The isotopomer in which the five NHs have been replaced by deuterium were prepared by repeated recrystallization from ethanol-*O-d*. 1-Methyl-*d*₃ cytosine

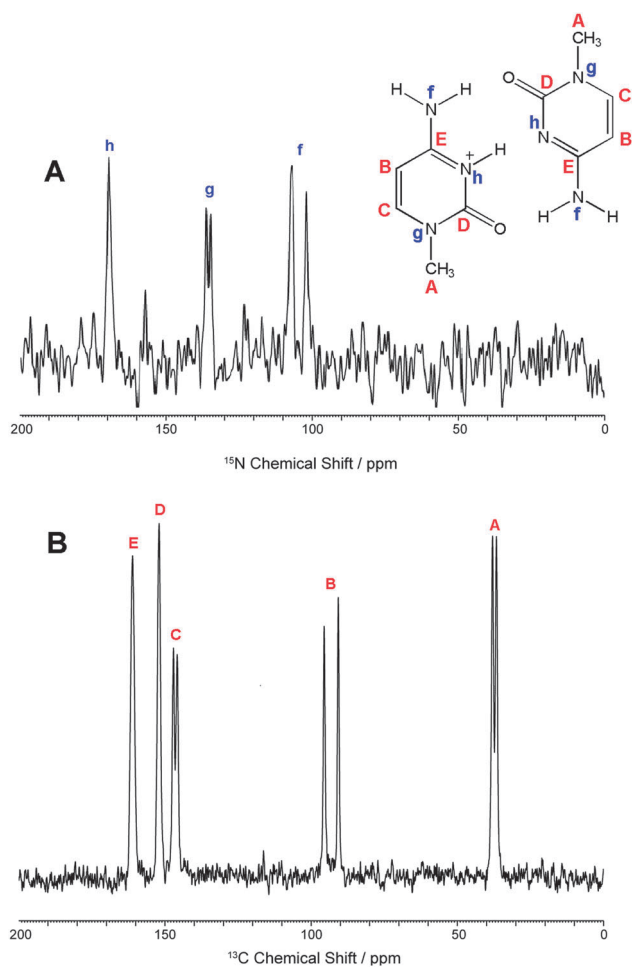


Fig. 2 (A) Solid phase ¹⁵N NMR (40.5 MHz) of the proton bound dimer of 1-methylcytosine, **1**, as its iodide salt; (B) ¹³C ssNMR (100.6 MHz) of the iodide salt of **1** (crystal habit B). For more detailed assignments see ESI,† Fig. S10 and S11.

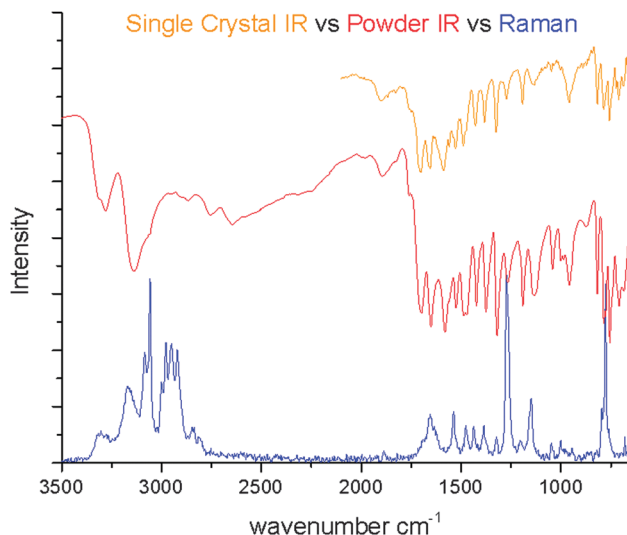


Fig. 3 Single crystal IR of the B form of the iodide salt of the proton bound dimer of 1-methylcytosine (shown in orange), powder IR spectrum of a mixture of polymorphs A and B (shown in red), and FT-Raman of a powder (in blue, 1064 nm exciting line).

was prepared using a method previously described⁶ but with CD₃I in place of CH₃I.

Magic angle spinning (MAS) solid state NMR (ssNMR) experiments were performed at 14.1 T (¹H frequency 600.01 MHz) on a Bruker AVANCE III spectrometer equipped with a triple-resonance 1.3 mm Biosolids (¹H/¹³C/¹⁵N) MAS probe, spinning at a MAS rate of 50 kHz. Solid state proton spectra were generated by Fourier transformation of a time-domain FID in response to a 3 μs excitation pulse, with 8192 complex time-domain data points digitized with a dwell of 40 μs (spectral width 25 kHz, total acquisition time 328 ms). 16 transients were averaged with a recycle delay of 3 s. Water served as an external standard calibrated to the chemical shift of TMS. The peaks in the proton ssNMR all have approximately the same linewidth (568 ± 174 Hz full width at half maximum).

¹³C cross-polarization (CP) MAS ssNMR experiments were performed at 14.1 and 9.4 T (¹H frequency 600.01 and 400.37 MHz respectively) using a double-resonance 4 mm MAS probe, spinning at a MAS rate of 8 kHz. 9.4 T experiments were performed on the Bruker AVANCE III spectrometer equipped with a double-resonance 2.5 mm MAS probe, spinning at a MAS rate of 20 kHz. 83 kHz ¹H π/2 and decoupling pulses were used along with a 2 ms CP and high power (83 kHz) ¹H decoupling during acquisition. During CP the ¹³C nutation rate was set to 41 kHz and the ¹H nutation rate ramped from 58–77 kHz. For each spectrum, 2048 complex data points with a dwell of 20 μs (spectral width 50 kHz, total acquisition time 41 ms) were acquired with a recycle delay of 3 s (14.1 T) and 4 s (9.4 T). ¹⁵N CP-MAS experiments on the iodide salt of **1** were performed at 9.4 T as described above, with 1024 complex data points with a dwell of 30 μs (spectral width 33.3 kHz, total acquisition time 30 ms) acquired with a recycle delay of 4 s. During CP the ¹⁵N nutation rate was set to 50 kHz and the ¹H nutation rate ramped from 58–77 kHz. ¹⁵N CP-MAS of the neutral and protonated monomers were performed at 14.1 T under conditions described above.

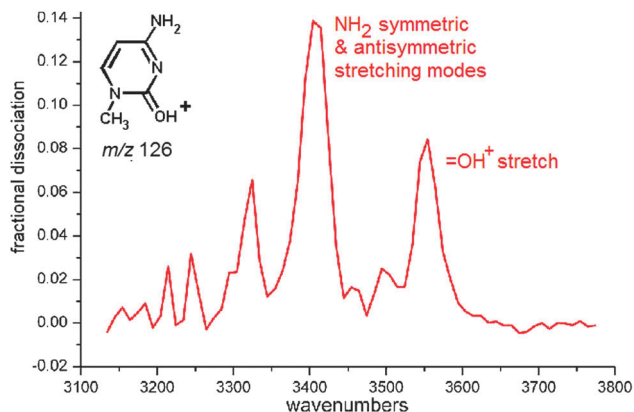


Fig. 4 Gas phase IRMPD spectrum of the O-protonated 1-methylcytosine monomer produced by electrospray from methanol–water showing OH and NH bands. Ion decomposition monitored by NH_3 loss from the protonated parent ion at m/z 126.

DFT calculations used the Gaussian09 program suite. Unless otherwise specified, geometry optimizations and normal modes computations were performed at the B3LYP/6-31G** level, with a scaling factor of 0.97 applied to normal mode frequencies above 800 cm^{-1} . GIAO calculations of NMR chemical shifts were performed on the gaseous ions. Barrier top geometries were optimized by imposing C_{2h} symmetry on the proton-bound homodimers.

Infrared powder spectra were recorded on an Perkin-Elmer One FT-ATR, Raman (1064 nm exciting line) on a Thermo Scientific Nicolet 6700 FT-IR with an NXR FT-Raman module, and single crystal IR on a Bruker Equinox 55 equipped with a microscope.

The techniques for IR multiple photon dissociation (IRMPD) spectroscopy of gaseous ions have been described in detail elsewhere.¹⁴ Briefly, ions electrosprayed from a $\approx 1\text{ mM}$ solution in methanol–water containing a trace of acetic acid were injected into a home-built 4.7 T Fourier-transform ion-cyclotron resonance mass spectrometer *via* a quadrupole deflector and a 1 m long RF octopole ion guide. IRMPD spectra were monitored by expulsion of neutral fragments as well as by diminution of the intensity of the protonated parent ions or proton-bound dimer ions as a function of IR wavelength. Infrared radiation was produced either from a free-electron laser (in the domain $\leq 1800\text{ cm}^{-1}$) or a LaserVision benchtop optical parametric oscillator (OPO) laser (in the domain $2450\text{--}3800\text{ cm}^{-1}$, whose maximum output is 20 mJ per pulse with a 10 Hz repetition rate). In cases where the extent of ion decomposition from irradiation in the $2450\text{--}3800\text{ cm}^{-1}$ domain was difficult to observe using the OPO by itself (Fig. 4 and the blue trace in Fig. 5), output from a 30 watt cw CO_2 laser was used to irradiate the sample immediately after the pulse from the tunable laser (OPO).

Results

The data presented here embrace a variety of experimental and computational approaches. As reported below, X-ray analysis indicates two stable crystal habits (called A and B) of the iodide

salt of **1**, only one of which (form A) has been previously described. Ascertaining the symmetry of proton-bound dimer **1** at room temperature for form B represents one objective, which ssNMR resolves in favor of a structure where the bridging proton does not lie midway between the nitrogens. Similarities between vibrational spectra in the crystalline and the gas phases suggest that the dimer has the same molecular symmetry in both states of matter. While IR and Raman of crystals and IRMPD vibrational spectroscopy of gaseous **1–6** provide evidence for that interpretation, they reveal that DFT calculations of normal modes do not give an accurate picture of the motion of the bridging proton from one nitrogen to the other. A brief summary of computational results serves to introduce the experimental data.

Computational results

Previous investigators have calculated the barrier to proton transfer within the gaseous proton-bound dimer of cytosine.¹¹ The potential surface for predicting vibrational frequencies makes use of the electronic energy barrier, while estimation of the enthalpy of activation includes a correction for the zero point energy difference between the equilibrium structure (C_s symmetry with 3N-6 modes) and the barrier top (C_{2h} symmetry having 3N-7 modes with positive force constants). B3LYP/cc-pVTZ optimizations for **1** and the barrier top give an electronic energy barrier of $4.50\text{ kcal mol}^{-1}$, which diminishes to $1.87\text{ kcal mol}^{-1}$ with application of a $2.63\text{ kcal mol}^{-1}$ zero point energy correction, comparable to previously published results.¹¹ An electronic energy difference of $5.27\text{ kcal mol}^{-1}$ results from single point calculations at CCSD/cc-pVTZ//B3LYP/cc-pVTZ. Experimental data from vibrational spectroscopy reported below suggest that normal modes calculations may seriously overestimate the zero point energy for the equilibrium geometry, owing to their inability to provide a reliable approximation for double-well potentials having low barriers. In any event, the calculated electronic energy barrier has a value higher than the harmonic zero point energy for the vibration having the highest degree of $\text{NH}\cdots\text{N}$ asymmetric stretch character (for which the normal modes calculation predicts an unscaled frequency of 2737 cm^{-1} at B3LYP/cc-pVTZ).

The calculated barrier for proton transit differs among the homodimers. The B3LYP/6-31G** electronic energy barriers for proton transfer between partners in proton-bound homodimers **1**, **2**, and **3** have values of 3.73, 3.25, and $3.90\text{ kcal mol}^{-1}$, respectively (as compared with the literature value for the proton-bound dimer of cytosine itself of $4.62\text{ kcal mol}^{-1}$ at that level¹¹). As noted in the previous paragraph, enlarging the basis set increases the calculated barrier.

Apart from the aforementioned motion in a double well potential, scaled normal mode frequencies give a good fit to observed IR and Raman bands, as will be outlined below. In other words, for each of the homodimers only one experimental band fails to match closely any of the calculated peaks, and this band vanishes in the gaseous ions with a D^+ bridge. That outcome leads to assignment of the supernumerary band in the fingerprint region of the H^+ bridged ions to the motion

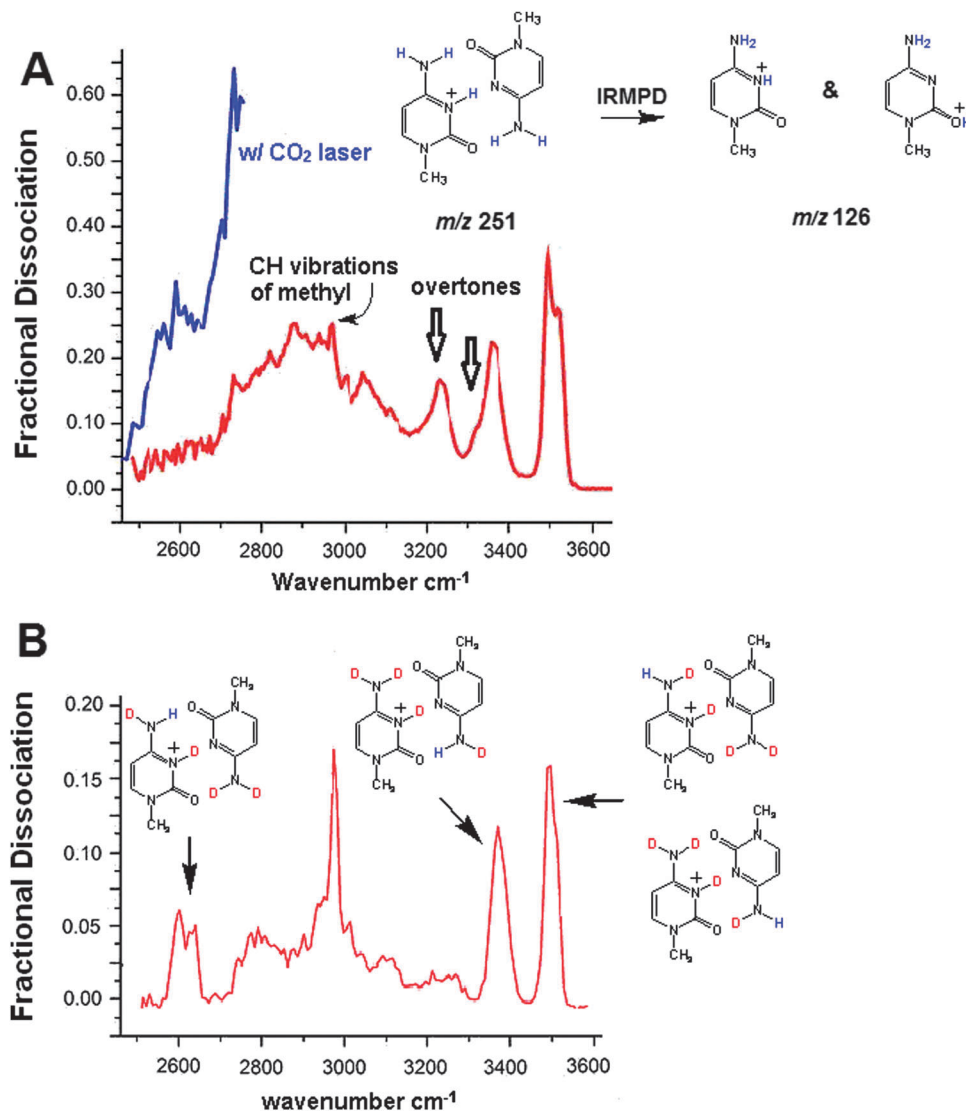


Fig. 5 IRMPD spectra of undeuterated proton-bound dimer cations from 1-methylcytosine (panel A, electrosprayed from water–methanol) and of the mixture of d_4 isomers (panel B, m/z 255 isolated from cations electrosprayed from D_2O – CH_3OD). The blue trace in panel A depicts the sensitivity improvement when an added pulse from a CO_2 laser increases the extent of multiple photon dissociation. The band near 3000 cm^{-1} vanishes upon methyl perdeuteration (see ESI†). The 2 dashed arrows in panel A indicate bands assigned to harmonics/combination bands on the basis of comparison with panel B.

having the greatest contribution from asymmetric $NH\cdots N$ stretch character.

Experimental results

Repeated recrystallizations of salts of the proton-bound dimer of 1-methylcytosine from absolute ethanol yield two different crystalline compounds, depending on whether an excess of molecular iodine is present. On one hand, the triiodide salt of **1** (black needles) contains two molecules of water for every proton-bound dimer. Cursory X-ray analysis of a polycrystalline sample indicates that it crystallizes in the $P2(1)/c$ space group. On the other hand, the mono-iodide salt of **1** contains no water but exists as a mixture of colorless polymorphs, one of which (crystal habit A) has the same unit cell dimensions as the previously reported structures (monoclinic P; $a = 7.1788\text{ \AA}$,

$b = 8.6098\text{ \AA}$, $c = 11.4628\text{ \AA}$, β angle = 97.241° at 100 K),⁶ while the other (crystal habit B) exhibits a monoclinic C-centered cell ($a = 20.430\text{ \AA}$, $b = 6.473\text{ \AA}$, $c = 13.064\text{ \AA}$, β angle = 125.395° at 100 K). The two crystal habits of the mono-iodide differ: A forms flakes, while B forms small needles.

Solid state NMR (ssNMR) spectra of a sample of the mono-iodide salt of **1** that contains predominantly the B form shows five proton resonances. The furthest downfield occurs at 16.1 ppm (see ESI†), which matches almost exactly the chemical shift predicted by GIAO calculations for the bridging proton in between the two ring nitrogens. The solid-phase probe does not have a wide range of temperature variability, but the proton ssNMR near 50°C is superimposable upon the one at room temperature.

Were the bridging proton held midway between two ring nitrogens, with r_{NO} equal to r_{ON} , the proton NMR should

Table 1 CP-MAS ^{13}C and ^{15}N chemical shifts (ppm) of crystalline samples of the iodide salt of **1** and its monomeric constituents at 150.87 MHz (carbon), 40.5 MHz (nitrogen) for the iodide salt of **1**, and 60.8 MHz (nitrogen) for neutral 1-methylcytosine and the iodide of its conjugate acid. External standard for carbon is adamantane referenced to TMS. External standard for nitrogen is ammonium chloride referenced to liquid ammonia

	Neutral MeCyt	Conjugate acid iodide salt	Proton-bound dimer monoiodide salt
Carbon			
Methyl	40.0	42.8	39.5, 40.8
C5 vinyl	94.9	92.6	93.6, 98.4
C6 vinyl	147.5	148.3	148.7, 150.0
Carbonyl	157.5	152.8	155.0
C-NH ₂	168.7	159.8	163.7, 164.2
Nitrogen			
N-Me	139.7	144.0	135.2, 136.4
H ₂ N	93.6	101.2	102.6, 107.7
Ring N	207.8	147.3	169.7

exhibit only five resonances, as observed. However, heteronuclear NMR demonstrates that the iodide salt of **1** does not possess such a high degree of symmetry. Fig. 2 reproduces the ^{13}C and ^{15}N ssNMR spectra of the sample. The resonances predicted for the isolated dimer cation in the gas phase enable the assignments summarized in Fig. 2. Table 1 lists the ^{13}C and ^{15}N chemical shifts and assignments for the constituent monomers as well as for the proton-bound dimer.

IR of a single needle containing predominantly the B form displays the 600–2000 cm^{-1} absorption profile reproduced at the top of Fig. 3, which exhibits slightly better resolution than the powder spectra of a mixture containing both polymorphs, of which both the IR and Raman are also reproduced. As noted above, a previous report cites one absorption as having special importance:¹³ the broad band with medium intensity at 1890 cm^{-1} , which appears in the IR of the iodide salt of **1** and also as a weak band in the Raman spectrum, shifted slightly to the red. This band persists with unchanged intensity in the IR of the salt in which all NHs have been exchanged for deuteria (see ESI[†]), which argues against its assignment as an NH stretch. An absorption near 1570 cm^{-1} , assigned in the gas phase spectra below to the motion of the proton that bridges from one ring nitrogen to the other, appears as a shoulder in the IR of the iodide salt of **1** but does not show up in the Raman.

Our previously published IRMPD spectrum of gaseous **1** exhibits this 1570 cm^{-1} band, which disappears upon replacement of the five exchangeable hydrogens with deuterium. That result leads to the assignment of the band as having predominantly the character of the asymmetric stretching motion of the bridging proton between the two ring nitrogens (the red H in Fig. 1B).¹⁷ Because of the difficulty of accessing frequencies above 1850 cm^{-1} at the free-electron laser beam setting used here, it has not yet proven possible to see if the gaseous ion also exhibits an 1890 cm^{-1} band in the gas phase. Apart from the 1570 cm^{-1} band, which is weak in the IR of the crystalline salt and absent in its Raman, the bands observed by IRMPD spectroscopy of the gaseous ion occur at nearly the same

frequencies as the IR absorptions of the solid (see ESI[†]). The spectra reproduced in Fig. 5 below permit assignment of the other NH stretches in the gaseous ion **1**.

IRMPD of the gaseous proton-bound homodimer of 1-methylcytosine, **1**, leads to expulsion of a neutral 1-methylcytosine molecule. The protonated monomer (m/z 126) that remains consists of a mixture of *O*-protonated and *N*-protonated monomers, as previously reported,¹⁷ despite the fact that the parent proton-bound dimer must be exclusively protonated on the ring nitrogen (as drawn for the m/z 251 ion in Fig. 5 as well as in Chart 1). The published IRMPD spectrum of the m/z 126 fragment from dissociation of the dimer exhibits a profile identical to that of the protonated monomer ion produced directly by electrospray from aqueous solution.¹⁷

IRMPD spectroscopy of the protonated monomer in the 3150–3800 cm^{-1} domain, reproduced in Fig. 4, shows a prominent band at 3555 cm^{-1} , confirming the presence of the *O*-protonated structure, as previously inferred from IRMPD spectra of the protonated monomer in the finger-print region.²⁰ The frequency is very close to the that of the OH stretch of the carboxyl group in protonated Ala-Ala as well as to the C=O-H band predicted for *O*-protonated formamide.²¹

In order to assign the NH vibrations of gaseous **1** it becomes necessary to look at a partially deuterated ion. The IRMPD spectrum of the undeuterated proton-bound homodimer **1** displays more bands in the 2500–3650 cm^{-1} domain than one might expect (Fig. 5). The spectrum was recorded under two conditions, one using only the output from a tunable OPO laser to dissociate the ions (red trace in panel A) and the other with an additional pulse from a CO₂ laser to enhance dissociation (blue trace in panel A). The blue trace shows a pair of absorption bands at 2560 and 2600 cm^{-1} that barely emerge from the noise level, which compares with a single absorption predicted at B3LYP/6-31G** of 2815 cm^{-1} (harmonic frequency scaled by 0.97), corresponding to the stretch of the hydrogen-bonded proton of the NH₂-group of the positively charged partner. Neither scaled normal modes at B3LYP/6-311++G** nor unscaled anharmonic frequencies (at B3LYP/6-31G** and at B3LYP/6-311++G**) match band positions any better,¹⁹ so this paper compares experimental vibrational band positions with scaled B3LYP/6-31G** normal modes throughout.

To clarify the spectra, as well as to diminish harmonics and combination bands, the experiment was repeated by electro-spraying the ions from D₂O-methanol-*O-d* and isolating the d_4 ions for IRMPD spectroscopy, as panel B shows. Such an experiment would present serious challenges in condensed phase spectroscopy, but in a gas phase study isolation of an ion possessing a designated m/z value becomes straightforward. While complete replacement of the five exchangeable hydrogens with deuterium produces a d_5 ion, the object of this experiment was to observe the spectra of a mixture of the four d_4 isomers drawn in panel B. Two bands that are not fundamentals (indicated by the open arrows in panel A) disappear in the d_4 spectra. Six prominent bands remain in the domain above 2500 cm^{-1} : the two bands assigned to the non-hydrogen bonded NH stretches near 3500 cm^{-1} (not as well resolved in

the d_4 spectra in panel B as in panel A; predicted for the d_0 at 3552 and 3595 cm^{-1} and for two of the d_4 isomers at 3550 and 3580 cm^{-1} , respectively), the NH stretch just below 3400 cm^{-1} corresponding to the hydrogen bonded amino group belonging to the uncharged partner in the dimer (predicted at 3360 cm^{-1} for **1** and at 3385 cm^{-1} for one of the d_4 isomers), the CH stretches of the methyl groups just below 3000 cm^{-1} , and a pair of bands near 2600 cm^{-1} corresponding to the hydrogen bonded amino group of the charged partner in the dimer. The frequency of this pair of bands shifts slightly to the blue in panel B (2600 and 2640 cm^{-1}) relative to panel A, but the separation between them remains approximately 40 cm^{-1} . As noted above, DFT predicts a single band at 2815 cm^{-1} for **1**, as compared with a single band predicted at 2830 cm^{-1} for one of the d_4 isomers. The experimental result would appear to rule out tunneling splitting as a cause of the doubling of this absorption. One possibility, discussed below, invokes a combination band with a butterfly vibration of the two rings. The NH...N stretch of the bridging proton between the two ring nitrogens, which DFT calculations predict at much higher frequencies than observed, occurs at a much lower frequency, as noted above.

Examination of the proton-bound dimer of 1-methyl- d_3 -cytosine, in which the 3000 cm^{-1} band vanishes (ESI⁺), provides confirmation of the assignment of the methyl CH band. With the exception of the 1570 cm^{-1} band, the observed band positions agree not only with predictions from scaled DFT normal modes calculations, but also with the positions of the absorptions of the solid salt in Fig. 3 (ESI⁺).

Looking at the IRMPD spectra of homodimers **2** and **3** reveals many of the same features seen in the published IRMPD spectrum of ion **1** in the fingerprint region.¹⁷ Rather than show the published spectra of **1** once again, this paper reproduces the IRMPD spectra of **2** and **3** and the d_5 -analogues from replacement of all the exchangeable hydrogens with deuterium.

Fig. 6–8 reproduce gas phase IRMPD spectra of the proton-bound homodimers of substituted analogues of 1-methylcytosine: 5-fluoro-1-methylcytosine (**2**) and 1,5-dimethylcytosine (**3**) and their deuterated analogues.

Fig. 6 compares the spectra of undeuterated **2** with a scaled B3LYP/6-31G** normal modes calculation, while Fig. 7 provides a comparison of the d_5 dimer produced by electrospray from D₂O–methanol- $O-d$ with the same level of DFT. Fig. 7 displays a good fit between experimental and calculated band positions in the 1000–1800 cm^{-1} domain, but Fig. 6 exhibits strong bands that do not coincide with theory. As noted above, the spectra in the 1000–1800 cm^{-1} domain closely resemble the previously published IRMPD spectra of **1** and its d_5 -analogue in the same domain.¹⁷ The extra bands in the 3200–3300 cm^{-1} domain of **2** are assigned to the same type of overtones as indicated by an open arrow in Fig. 5A. The extra band in the 1000–1800 cm^{-1} domain is assigned to a fundamental at 1580 cm^{-1} corresponding to the NH...N stretch between the two ring nitrogens.

For homodimer **3**, comparing experiment with theory for the deuterated d_5 -dimer in lower panel of Fig. 8 again shows an excellent fit between observed and predicted band positions, while the upper panel of Fig. 8 again exhibits a poorer fit between experiment and the DFT normal modes. In looking at Fig. 6–8, it becomes apparent that both homodimers **2** and **3** display one extra peak in the 1500–1600 cm^{-1} domain beyond what theory predicts. As in the case of the previously published IRMPD spectra of **1**, the extra peak is assigned to the stretching vibration of the bridging proton (the H shown in red in Fig. 1B).

Fig. 9–11 reproduce the IRMPD spectra of the three proton-bound heterodimers **4–6** that can be formed from 1-methylcytosine and its aforementioned analogues. Once again, comparing experimental spectra with DFT normal modes calculations show more experimental bands than DFT predicts. In Fig. 10 and 11, overtones occur in the 3200–3300 domain, just as observed in Fig. 5A and 6. And, once again, extra peaks occur in the

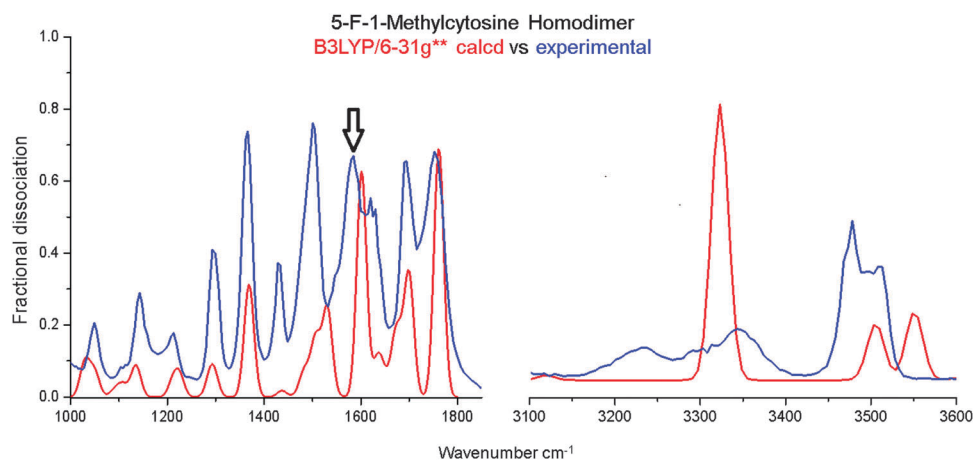


Fig. 6 IRMPD spectra of ion **2** recorded using a free-electron laser (blue trace, left hand panel) and an OPO laser (blue trace, right hand panel) compared with normal mode frequencies calculated at B3LYP/6-31G** (red traces, scaled by 0.97; 30 cm^{-1} Gaussian broadening). On the basis of Fig. 5, the band observed around 3230 cm^{-1} and the shoulder at 3300 cm^{-1} are assigned as overtones. Following Fig. 5, the band around 3350 cm^{-1} is assigned to the stretch of the hydrogen-bonded NH from the primary amino group of the uncharged partner and the 3470–3520 cm^{-1} bands to the non-hydrogen-bonded NHs of the primary amino groups. The arrow indicates the band in the fingerprint region assigned to motion of the bridging H⁺.

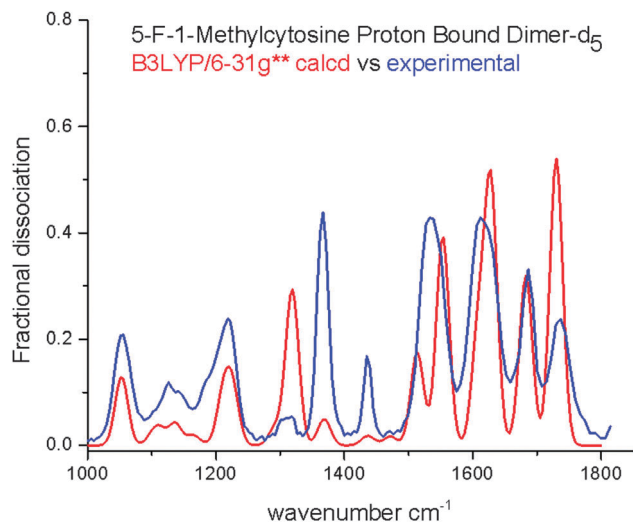


Fig. 7 IRMPD spectra of the d_5 analogue of ion **2** from replacement of the exchangeable hydrogens with deuterium (blue trace recorded using the free-electron laser) compared with normal mode frequencies calculated at B3LYP/6-31G** (red trace, scaled by 0.97; 30 cm^{-1} Gaussian broadening).

$1500\text{--}1600\text{ cm}^{-1}$ domain in all of the heterodimers. The existence of two tautomers of the heterodimers provides a possible explanation, which the Discussion section below will briefly address.

Discussion

The symmetry of the proton-bound dimer of cytosine and its derivatives has occasioned much discussion.^{6,7} The ^{13}C and ^{15}N solid state NMR spectra of solid samples of the iodide salt of the proton-bound dimer of 1-methylcytosine, **1**, (predominantly the B crystal habit) confirm the asymmetry of the dimer at room temperature. The bridging proton preferentially associates with one or the other of the two ring nitrogens, as Fig. 1B illustrates, permitting differentiation between the charged and the uncharged partners in dimer ion **1**. Vibrational spectroscopy of gaseous ion **1** at ambient temperature and the IR of its crystalline iodide salt show such similarities as to suggest that **1** has the same structure in both phases.

The widths of solid phase NMR absorptions ($>100\text{ Hz}$, even with magic angle spinning) preclude measurement of scalar spin-spin coupling constants and also make it difficult to separate closely spaced resonances. On one hand, the proton NMR of the crystalline iodide salt of **1** shows only five peaks, possibly consistent with a symmetric structure. On the other hand, heteronuclear solid phase NMR spectra (^{15}N and ^{13}C) display five and eight peaks, respectively, which require the dimer to have an asymmetric structure with $r_{\text{NO}} \neq r_{\text{ON}}$ at room temperature. If the dimer did have C_2 symmetry, only three ^{15}N and five ^{13}C peaks should have been seen.

The ^{15}N natural abundance NMR exhibits smaller differences than predicted by DFT for the gaseous cation. The two primary amino groups exhibit a difference of 5.5 ppm (calculated 14 ppm; see ESI†) and are both downfield of the experimental values for the neutral and protonated monomers. A 6 ppm difference

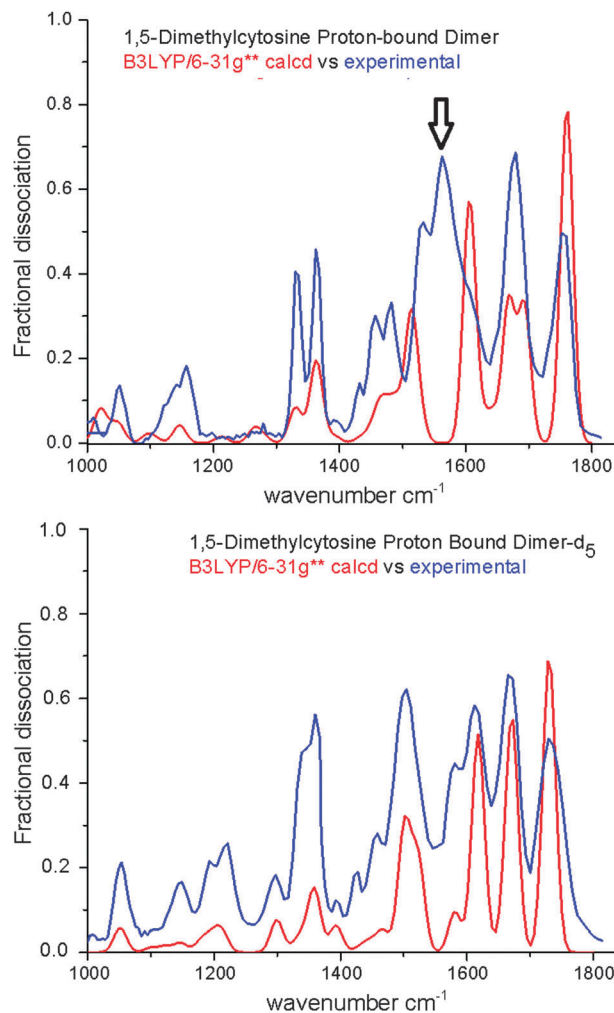


Fig. 8 IRMPD spectra of ion **3** recorded using the free-electron laser (blue trace, top panel) and its d_5 analogue from replacement of the exchangeable hydrogens with deuterium (blue trace, bottom panel) compared with normal mode frequencies calculated at B3LYP/6-31G** (red traces, scaled by 0.97; 30 cm^{-1} Gaussian broadening). The arrow in the upper panel indicates the band in the fingerprint region assigned to motion of the bridging H^+ .

separates the resonances of the methylated ring nitrogens (calculated 9 ppm), which are both upfield from the experimental values for the neutral and protonated monomers. The resonances of proton-bridged ring nitrogens overlap one another and have a value nearly equal to the algebraic mean of the experimental values for neutral and monoprotonated monomers. Although the literature reports that, in the hydrated iodide salt of **1**, ^{14}N nuclear quadrupole resonance distinguishes between the proton-bridged ring nitrogens,²² this proves not to be the case in the ^{15}N NMR experiments reported here. Although the charged and uncharged partners remain distinct in the anhydrous iodide salt of **1**, NMR resolves neither the two proton-bridged ring nitrogens nor the two carbonyl carbons.

In the ^{13}C NMR a difference of 1.3 ppm separates the two methyl resonances of the iodide salt of **1**, substantially greater than theory predicts for the gaseous ion (a difference of only 0.2 ppm; see ESI†) but less than the difference between the

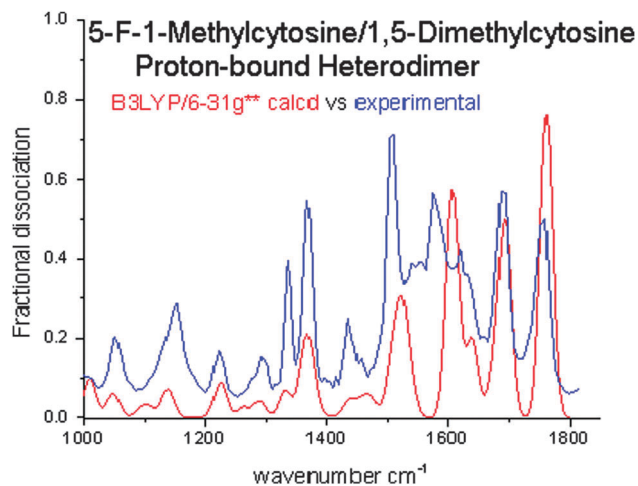


Fig. 9 IRMPD spectra of proton-bound heterodimer **4** recorded using a free-electron laser (blue trace) compared with normal mode frequencies calculated at B3LYP/6-31G** (red trace, scaled by 0.97; 30 cm^{-1} Gaussian broadening). In all three homodimers **1–3** and in all three heterodimers, **4–6**, the highest frequency band in this domain (between 1750 and 1760 cm^{-1} in all cases) corresponds to the carbonyl stretch combined with an in-plane bend of the $\text{NH}\cdots\text{N}$ hydrogen that bridges between the two ring nitrogens. At least one band is seen in the 1500 – 1600 cm^{-1} domain not predicted by the normal modes calculation.

neutral precursor and the iodide salt of its conjugate acid (2.6 ppm). The upfield pair of vinyl resonances displays an opposite trend: a difference of 4.8 ppm separates the upfield pair of the proton-bound homodimer, as compared with a calculated difference 2.0 ppm and an experimental difference between neutral and conjugate acid of 2.4 ppm (with the neutral resonance more downfield). The downfield pair of vinylic carbons exhibits much better agreement with theory: an experimental difference of 1.3 ppm separates the pair from the homodimer, as compared with a calculated difference of 1.2 ppm and an experimental difference between neutral and

conjugate acid of 0.8 ppm. The aminated carbons provide the furthest downfield absorptions, separated by only 0.4 ppm, versus a predicted difference of 5.2 ppm and an experimental separation between neutral and conjugate acid of 8.9 ppm. The separation of the two carbonyl resonances from the dimer is less than the resolution of the instrument, while the predicted difference has a value of 8.8 ppm and the experimental separation between neutral and conjugate acid has a value of 4.7 ppm (with the neutral farther downfield). The disagreements between computation and theory suggest that, in the solid salts, interactions between the cations and the iodide counterion affect shielding.

Previous work has highlighted discrepancies between the normal modes approximation and experimental results for double well potentials.¹⁶ Double wells for proton-bridged conjugate acid ions with much simpler structure have been solved in reduced dimensionality. When the electronic energy barrier has a value comparable to the zero point energy for intramolecular proton transfer, observed $\nu = 0 \rightarrow \nu = 1$ transitions for $\text{N-H}\cdots\text{N}$ transit have much lower values (550 – 600 cm^{-1}) than normal mode calculations predict (even with anharmonic corrections). In the present case, the electronic energy for the double-well potential of **1** has a value higher than the anticipated zero point energy, yet the observed vibrational transitions for **1–6** (around 1570 cm^{-1}) still exhibit frequencies lower than expected on the basis of DFT normal modes.

The IR absorption spectrum of the crystalline iodide salt of **1** shows a band at the same frequency as previously reported at 1890 cm^{-1} (ref. 13) as well as a shoulder near 1570 cm^{-1} , the band assigned to the $\text{NH}\cdots\text{N}$ stretch in the gaseous ions. Deuterium substitution of a crystalline sample argues against assignment of the 1890 cm^{-1} band as an NH stretch, but the range of the free-electron laser used for the gas phase IRMPD spectra does not extend far enough to see if the 1890 cm^{-1} band also occurs in the gaseous ion. The IRMPD spectrum of **1** in the

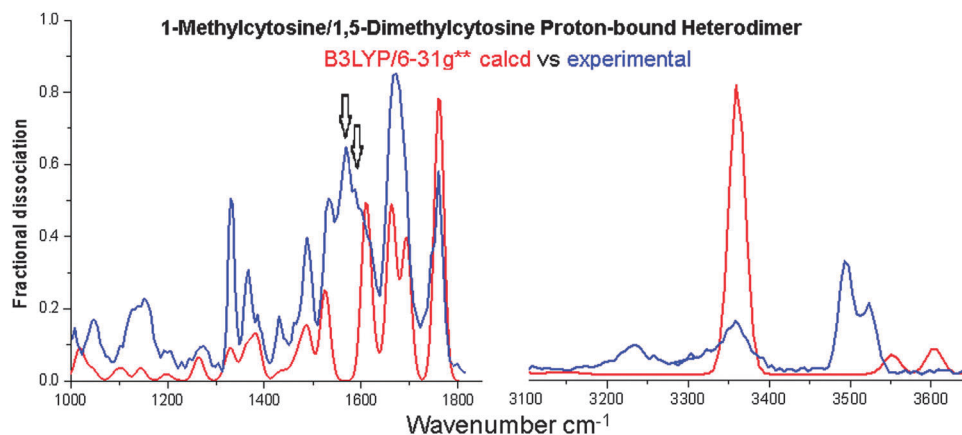


Fig. 10 IRMPD spectra of proton-bound heterodimer **5** recorded using a free-electron laser (blue trace, left hand panel) and an OPO laser (blue trace, right hand panel) compared with normal mode frequencies calculated at B3LYP/6-31G** (red traces, scaled by 0.97; 30 cm^{-1} Gaussian broadening). On the basis of Fig. 5, the band observed around 3230 cm^{-1} and the shoulder near 3300 cm^{-1} are assigned as overtones. Following Fig. 5, the band around 3350 cm^{-1} is assigned to the stretch of the hydrogen-bonded NH from the primary amino group of the uncharged partner and the 3500 – 3530 cm^{-1} bands to the non-hydrogen-bonded NHs of the primary amino groups. At least two bands are seen in the 1500 – 1600 domain not predicted by the normal modes calculation, as indicated by the two arrows in the fingerprint region.

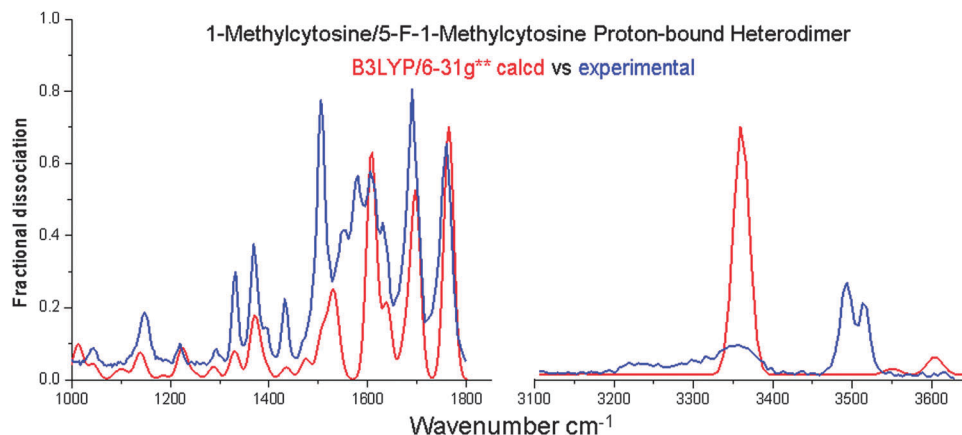


Fig. 11 IRMPD spectra of proton-bound heterodimer **6** recorded using a free-electron laser (blue trace, left hand panel) and an OPO laser (blue trace, right hand panel) compared with normal mode frequencies calculated at B3LYP/6-31G** (red traces, scaled by 0.97; 30 cm⁻¹ Gaussian broadening). On the basis of Fig. 5, the band observed around 3230 cm⁻¹ and the shoulder near 3300 cm⁻¹ are assigned as overtones. Following Fig. 5, the band around 3350 cm⁻¹ is assigned to the stretch of the hydrogen-bonded NH from the primary amino group of the uncharged partner and the 3490–3520 cm⁻¹ bands to the non-hydrogen-bonded NHs of the primary amino groups. At least one band is seen in the 1500–1600 domain not predicted by the normal modes calculation.

fingerprint region has been previously published¹⁷ and shows such great similarities to the spectra of gaseous homodimers **2** and **3** that Table 2 summarizes the assignment without the spectrum having to be reproduced here a second time.

The IRMPD spectrum of gaseous **1** in the NH stretching region (Fig. 5) exhibits a band from the NH₂ hydrogen of the uncharged partner that enjoys hydrogen bonding with the carbonyl oxygen of the charged partner (3380 cm⁻¹) and a separate band from the NH₂ hydrogen of the charged partner that enjoys hydrogen bonding with the carbonyl oxygen of the uncharged partner (2560 cm⁻¹ with a band of nearly equal intensity 40 cm⁻¹ to the blue). Table 2 summarizes assignments for the NH stretches of proton-bound homodimers in the gas phase. The stretch of the hydrogen bonded NH₂ hydrogen of the neutral partner in ion **2** occurs at a slightly lower frequency (3345 cm⁻¹), as predicted by DFT (a 7 cm⁻¹ calculated red shift at B3LYP/6-31G**), corresponding to an NH distance 0.004 Å longer than calculated for **1**. At the same time the NH...N stretch between the two ring nitrogens in **2** occurs at a slightly higher frequency (1580 cm⁻¹), corresponding to a distance between ring nitrogens 0.026 Å shorter than calculated for **1**. Despite a calculated difference between r_{NO} and r_{ON} of 0.26 Å calculated for each of the homodimers (virtually the same as computed for **1** using the cc-pVTZ basis), DFT geometry optimization gives a N–H...N bond angle $\geq 179.5^\circ$ for the ionic hydrogen bond between the ring nitrogens.

With regard to IR spectroscopy, the bands observed in the powder spectrum agree well with the absorption spectrum of a

single needle of the B form. With the exception of the strong 1570 cm⁻¹ band in the previously published IRMPD spectrum of isolated **1**, all of the bands in the crystalline sample in the 500–1700 cm⁻¹ domain correlate with those in the gas phase IRMPD spectrum (see ESI[†]). Both the IRMPD spectrum of gaseous **1** and the IR absorption spectrum of the solid iodide salt display bands that must be assigned to harmonics or combination bands. The method of partial deuteration (Fig. 5) reduces the number of bands in the gas phase spectrum sufficiently that assignments can be made in the 2500–3500 cm⁻¹ domain, as the first column in Table 2 summarizes.

One combination band that partial deuteration of gaseous ion **1** appears not to remove is the higher frequency absorption of the pair of IRMPD bands near 2600 cm⁻¹. Although partial deuteration does shift this pair of bands, the 40 cm⁻¹ splitting does not change. A provisional assignment of the higher frequency band to a combination with the calculated 40 cm⁻¹ flapping motion of the two rings (also called a butterfly motion²³) seems probable. While IRMPD spectroscopy has not yet observed the 40 cm⁻¹ fundamental directly, vibronic spectroscopy of neutral molecules demonstrates the accuracy of unscaled normal modes for low frequency modes of ground electronic states when compared with the experimental values observed for electronically excited states.²⁴ For example, the lowest energy IR-active fundamentals of the neutral dimer of 1-methylcytosine with the enol form of cytosine have predicted harmonic frequencies of 30 and 48 cm⁻¹ (B3LYP/6-31G**), no

Table 2 Bands observed for NH stretches for gaseous homodimers **1–3** by IRMPD (cm⁻¹)

	1	2	3
Non H-bonded hydrogens of –NH ₂ groups	3500, 3520	3475, 3510	^a
–NH ₂ H-bonded hydrogen of uncharged ring	3380	3345	^a
–NH ₂ H-bonded hydrogen of charged ring	2560	^b	^a
H-bonded hydrogen between ring nitrogens	1570	1580	1560

^a Not recorded. ^b Too weak to observe.

more than 1–2 cm^{-1} away from the values from the reported vibronic spectrum of the neutral dimer in a hole-burning experiment.²⁵

The IRMPD spectra of the 5-fluoro and 5-methyl substituted homodimer cations **2** and **3** share nearly all of the features of the previously published spectrum of **1**, including a band near 1570 cm^{-1} that is not predicted by theory, which vanishes upon replacement of all five exchangeable protons with deuterium. One would expect such a band to shift upon isotopic substitution, but in no case is it possible definitively to assign a band in the spectra of the deuterated ions that corresponds to a shifted band. Such behavior has been noted previously in proton-bridged diamines,¹⁶ and it may be that the intensity of the bands corresponding to shifted absorptions of the d_5 -ions diminishes as a consequence of deuteration. In any event, just as in the published d_5 -homodimer of 1-methylcytosine (**1- d_5**), the experimental band positions give a good match to theory (scaled harmonic B3LYP/6-31G**) in the 1000–1800 cm^{-1} domains of the 5-fluoro-1-methylcytosine (Fig. 7) and 1,5-dimethylcytosine (Fig. 8) homodimers **2- d_5** and **3- d_5** . By contrast, overtones (unexpected based on the normal modes calculations) occur just above 3200 cm^{-1} in every spectrum examined using the OPO laser (homodimers in Fig. 5A and 6; heterodimers in Fig. 9 and 10). As theory predicts for isolated **1**, the vinylic CH stretching vibrations in the crystalline iodide salt of **1** display greater intensity relative to NH stretches in the Raman (Fig. 3) than they do in the IR.

The IRMPD spectra of all three proton-bound heterodimers (**4**, **5**, and **6**) in the 1000–1800 cm^{-1} domain appear more congested between 1500 and 1600 cm^{-1} than do the homodimer spectra. Occurrence of combination bands with very low frequency vibrations provides one possible explanation, analogous to the pair of bands near 2600 cm^{-1} in the IRMPD spectrum of **1**. An alternative interpretation holds that two tautomers of a heterodimer absorb at different frequencies for the ring NH proton, but exhibit the same absorptions everywhere else. Whereas transit of the bridging H^+ in a homodimer interchanges r_{NO} and r_{ON} , leading to an ion having the same structure, proton shift within a heterodimer produces a tautomeric ion with a different structure. Proton exchange between the charged and uncharged partners, particularly within heterodimer **5**, could lead to appreciable concentrations of two tautomers for a heterodimeric ion at ambient temperature, accounting for an increase in the observed number of bands. DFT calculations suggest that only 0.5 kcal mol^{-1} separates the two tautomers of **5** (*versus* 2.4 kcal mol^{-1} for **4** and 1.9 kcal mol^{-1} for **6**), both of which correspond to local minima.

Ring methylation affects binding. In biological systems, methylation at the 5-position of cytosine residues serves to repress gene transcription,²⁶ and it appears likely that cytosine methylation occurs in promoter regions as well as in genes. DFT predicts that pairing within the i-motif becomes weakened by methylation of one of the cytosines. Although computational methods consistently overestimate the binding of cytosine to its protonated parent¹¹ relative to the experimental value in the literature,²⁷ DFT predicts that the favored tautomer of heterodimer

5 has a binding enthalpy 0.6 kcal mol^{-1} less than calculated for homodimer **1**. Further investigation of proton-bound cytosine dimers can address substituent effects on binding and tautomeric equilibria in greater detail.

Acknowledgements

The authors are grateful to Dr Fook Tham for X-ray crystallographic analysis, Bryan Tamashiro and Prof. G. J. O. Beran for performing anharmonic frequency calculations, and to the FELIX staff for their skillful assistance in helping perform IRMPD experiments, particularly Dr A. F. G. van der Meer and B. Redlich. This work was supported by the NSF (CHE-0848607 to L.J.M. and CHE-0848517 to T.H.M.), by the Nederlandse Organisatie voor Wetenschappelijk Onderzoek (NWO), and by the CNRS. H.U.U. and R.A.K. gratefully acknowledge support through US Department of Education GAANN Award #P200A120170.

References

- (a) G. Biffi, D. Tannahill, J. McCafferty and S. Balasubramanian, *Nat. Chem.*, 2013, **5**, 182–186; (b) A. Siddiqui-Jain and L. H. Hurley, *Nat. Chem.*, 2013, **5**, 153–155; (c) E. Y. N. Lam, D. Beraldi, D. Tannahill and S. Balasubramanian, *Nat. Commun.*, 2013, **4**, 1796; (d) G. Biffi, D. Tannahill, J. McCafferty and S. Subramanian, *Nat. Chem.*, 2013, **5**, 182–186.
- (a) A. L. Lieblein, J. Buck, K. Schlepckow, B. Fürtig and H. Schwalbe, *Angew. Chem., Int. Ed.*, 2012, **51**, 250–253; (b) A. L. Lieblein, M. Krämer, A. Dreuw, B. Fürtig and H. Schwalbe, *Angew. Chem., Int. Ed.*, 2012, **51**, 4067–4070; (c) A. L. Lieblein, B. Fürtig and H. Schwalbe, *ChemBioChem*, 2013, **14**, 1226–1230.
- A. I. S. Holm, L. M. Nielsen, B. Kohler, S. Vronning Hoffmann and S. Brøndsted Nielsen, *Phys. Chem. Chem. Phys.*, 2010, **12**, 9581–9596.
- (a) D. E. Gilbert and J. Feigon, *Curr. Opin. Struct. Biol.*, 1999, **9**, 305–314; (b) D. Sun and L. H. Hurley, *J. Med. Chem.*, 2009, **52**, 2863–2874; (c) S. Kendrick, Y. Akiyama, S. M. Hecht and L. H. Hurley, *J. Am. Chem. Soc.*, 2009, **131**, 17667–17676; (d) J. Dai, A. Ambrus, L. H. Hurley and D. Yang, *J. Am. Chem. Soc.*, 2009, **131**, 6102–6104; (e) T. A. Brooks, S. Kendrick and L. H. Hurley, *FEBS J.*, 2010, **277**, 3459–3469; (f) J. Dai, E. Hatzakis, L. H. Hurley and D. Yang, *PLoS One*, 2010, **5**, e11647; (g) S. Dhakal, J. D. Schonhoft, D. Koirala, Z. Yu, S. Basu and H. Mao, *J. Am. Chem. Soc.*, 2010, **132**, 8991–8997; (h) J. A. Brazier, A. Shah and G. D. Brown, *Chem. Commun.*, 2012, **48**, 10739–10741; (i) C. E. Kaiser, V. Gokhale, D. Yang and L. H. Hurley, *Top. Curr. Chem.*, 2013, **330**, 1–22.
- (a) T. J. Kistenmacher, M. Rossi and L. G. Marzilli, *Biopolymers*, 1978, **17**, 2581–2585; (b) F. Fujinami, K. Ogawa, Y. Arakawa, S. Shirotake, S. Fujii and K.-I. Tomita, *Acta Crystallogr.*, 1979, **B35**, 968–970; (c) M. Gdaniec, B. Brycki and M. Szafran, *J. Chem. Soc., Perkin Trans. 2*, 1988, 1775–1779; (d) A. Schimanski, E. Freisinger, A. Erxleben and B. Lippert, *Inorg. Chim. Acta*, 1998, **283**, 223–232; (e) M. A. Salam and K. Aoki, *Inorg. Chim. Acta*, 2000, **311**, 15–24; (f) D. Armentano,

- G. De Munno, L. Di Donna, G. Sindona, G. Giorgi and L. Salvini, *J. Am. Soc. Mass Spectrom.*, 2004, **15**, 268–279;
- (g) T. Murata and G. Saito, *Chem. Lett.*, 2006, 1342–1343;
- (h) T. Murata, Y. Enomoto and G. Saito, *Solid State Sci.*, 2008, **10**, 1364–1368;
- (i) N. Bosnjaković-Pavlović, A. Spasajević-de Biré, I. Tomaz, N. Bouhaida, F. Avecilla, U. B. Mioc, J. C. Pessoa and N. E. Ghermani, *Inorg. Chem.*, 2009, **48**, 9742–9753.
- 6 (a) T. Krüger, C. Bruhn and D. Steinborn, *Org. Biomol. Chem.*, 2004, **2**, 2513–2516; (b) J. Müller and E. Freisinger, *Acta Crystallogr.*, 2005, **E61**, o320–o322.
- 7 N. Bosnjaković-Pavlović and A. Spasajević-de Biré, *J. Phys. Chem. A*, 2010, **114**, 10664–10675.
- 8 (a) R. Langridge and A. Rich, *Nature*, 1963, **198**, 725; (b) C. H. Kang, I. Berger, C. Lockshin, R. Ratliff, R. Moyzis and A. Rich, *Proc. Natl. Acad. Sci. U. S. A.*, 1994, **91**, 11636–11640; (c) I. Berger, C. H. Kang, A. Fredian, R. Ratliff, R. Moyzis and A. Rich, *Nat. Struct. Biol.*, 1995, **2**, 416–425; (d) C. H. Kang, I. Berger, C. Lockshin, R. Ratliff, R. Moyzis and A. Rich, *Proc. Natl. Acad. Sci. U. S. A.*, 1995, **92**, 3874–3878; (e) L. Cai, L. Chen, S. Raghavan, R. Ratliff, R. Moyzis and A. Rich, *Nucleic Acids Res.*, 1998, **26**, 4696–4705.
- 9 J. Weil, T. Min, C. Yang, S. Wang, C. Sutherland, N. Sinha and C. H. Kang, *Acta Crystallogr.*, 1999, **D55**, 422–429.
- 10 A. R. Moehlig, K. E. Djernes, V. Mahesh Krishnan and R. J. Hooley, *Org. Lett.*, 2012, **14**, 2560–2563.
- 11 S. Y. Han and H. B. Oh, *Chem. Phys. Lett.*, 2006, **432**, 269–274.
- 12 N. V. Hud and T. H. Morton, *J. Phys. Chem. A*, 2007, **117**, 3369–3377.
- 13 T. J. Kistenmacher, M. Rossi, J. P. Caradonna and L. G. Marzilli, *Adv. Mol. Relax. Interact. Processes*, 1979, **15**, 119–133.
- 14 (a) D. Oepts, A. F. G. van der Meer and P. W. Van Amersfoort, *Infrared Phys. Technol.*, 1995, **36**, 297–308; (b) J. J. Valle, J. R. Eyler, J. Oomens, D. T. Moore, A. F. G. van der Meer, G. von Helden, G. Meijer, C. L. Hendrickson, A. G. Marshall and G. T. Blakney, *Rev. Sci. Instrum.*, 2005, **76**, 023103; (c) N. C. Polfer and J. Oomens, *Phys. Chem. Chem. Phys.*, 2007, **9**, 3804–3817; (d) N. C. Polfer, *Chem. Soc. Rev.*, 2011, **40**, 2211–2221.
- 15 (a) C. Kapota, J. Lemaire, P. Maître and G. Ohanessian, *J. Am. Chem. Soc.*, 2004, **126**, 1836–1842; (b) D. T. Moore, J. Oomens, L. van der Meer, G. von Helden, G. Meijer, J. Valle, A. G. Marshall and J. R. Eyler, *ChemPhysChem*, 2004, **5**, 740–743; (c) T. D. Fridgen, L. MacAleese, P. Maître, T. B. McMahon, P. Boissel and J. Lemaire, *Phys. Chem. Chem. Phys.*, 2005, **7**, 2747–2755; (d) X. Li, D. T. Moore and S. S. Iyengar, *J. Chem. Phys.*, 2008, **128**, 184308; (e) X. Li, J. Oomens, J. R. Eyler, D. T. Moore and S. S. Iyengar, *J. Chem. Phys.*, 2010, **132**, 244301; (f) K. Rajabi, K. Theel, E. A. L. Gillis, G. Beran and T. D. Fridgen, *J. Phys. Chem. A*, 2009, **113**, 8099–8107.
- 16 (a) G. J. O. Beran, E. L. Chronister, L. L. Daemen, A. R. Moehlig, L. J. Mueller, J. Oomens, A. Rice, D. R. Santiago-Dieppa, F. S. Tham, K. Theel, S. Yaghmaei and T. H. Morton, *Phys. Chem. Chem. Phys.*, 2011, **13**, 20380–20392; (b) H. U. Ung, A. R. Moehlig, S. Khodagholian, G. Berden, J. Oomens and T. H. Morton, *J. Phys. Chem. A*, 2013, **117**, 1360–1369.
- 17 J. Oomens, A. R. Moehlig and T. H. Morton, *J. Phys. Chem. Lett.*, 2010, **1**, 2891–2897.
- 18 D. L. Helfer II, R. S. Hosmane and N. J. Leonard, *J. Org. Chem.*, 1981, **46**, 4803–4804.
- 19 A. R. Moehlig, PhD thesis, University of California, Riverside, 2011.
- 20 (a) J.-Y. Salpin, S. Guillaumont, J. Tortajada, L. MacAleese, J. Lemaire and P. Maître, *ChemPhysChem*, 2007, **8**, 2235–2244; (b) J. M. Bakker, J.-Y. Salpin and P. Maître, *Int. J. Mass Spectrom.*, 2009, **283**, 214–221.
- 21 (a) A. Cimas, T. D. Vaden, T. S. J. A. de Boer, L. C. Snoek and M.-P. Gaigeot, *J. Chem. Theory Comput.*, 2009, **5**, 1068–1078; (b) C.-C. Wu, J. C. Chang, I. Hahndorf, C. Chaudhuri, Y. T. Lee and H. C. Chang, *J. Phys. Chem. A*, 2000, **104**, 9556–9565.
- 22 Y. Hiyama, L. G. Butler, W. A. Olsen and T. L. Brown, *J. Magn. Reson.*, 1981, **44**, 483–487.
- 23 E. Nir, C. Janzen, P. Imhof, K. Kleinermanns and M. S. de Vries, *Phys. Chem. Chem. Phys.*, 2002, **4**, 740–750.
- 24 K. Song, A. van Eijk, T. A. Shaler and T. H. Morton, *J. Am. Chem. Soc.*, 1994, **116**, 4455–4460.
- 25 E. Nir, I. Hünig, K. Kleinermanns and M. S. de Vries, *Phys. Chem. Chem. Phys.*, 2003, **5**, 4780–4785.
- 26 (a) A. Razin and A. D. Riggs, *Science*, 1980, **210**, 604–610; (b) C. D. Warden, H. Lee, J. D. Tompkins, X. Li, C. Wang, A. D. Riggs, H. Yu, R. Jove and Y.-C. Yuan, *Nucleic Acids Res.*, 2013, DOI: 10.1093/nar/gkt242.
- 27 M. Meot-Ner (Mautner), *Chem. Rev.*, 2005, **105**, 213–284; M. Meot-Ner (Mautner), *Chem. Rev.*, 2012, **112**, PR22–PR103.